Vol. 38 (2007) ACTA PHYSICA POLONICA B No 4

EFFECT OF SHELL STRUCTURE ON SADDLE POINT MASSES*

W.J. Świątecki

Nuclear Science Division, Lawrence Berkeley National Laboratory
Berkeley, California 94720, USA

K. Siwek-Wilczyńska

Institute of Experimental Physics, Warsaw University
Hoża 69, 00-681 Warsaw, Poland

J. Wilczyński

The Andrzej Sołtan Institute for Nuclear Studies,
05-400 Otwock-Świerk, Poland

(Received October 19, 2006)

For nuclei in the range of atomic numbers from $Z = 71$ to $Z = 120$ we present a survey of experimental and theoretical deviations of ground state and fission saddle point masses from their respective macroscopic approximations. The mass deviations (related to shell effects) are an order of magnitude smaller for saddles than for ground states. This can be understood on the basis of the "topographic theorem".

PACS numbers: 21.10.Dr, 24.75.+i

1. Introduction

Measured nuclear ground state masses show large deviations from a smooth macroscopic (Liquid Drop type) approximation. The deviations, due to nuclear shell structure, reach as much as about -13 MeV for doubly magic nuclei, such as ^{208}Pb and ^{132}Sn. By contrast, measured masses of nuclei in their fission saddle-point configurations are much smoother functions of N and Z, the neutron and atomic numbers. (A measured saddle mass is

* Presented at the Zakopane Conference on Nuclear Physics, September 4–10, 2006, Zakopane, Poland.

the sum of the measured ground state mass and the measured fission barrier.) There are available today some 120 measured saddle masses, deduced from the 120 fission barriers listed in [1]. Fig. 1 shows both the ground-state and saddle-point deviations for 120 nuclei in the range $Z = 71$ to $Z = 100$. The plot is against the neutron number N with lines connecting isotopes. Later I will also discuss some 300 preliminary *theoretical* estimates of saddle masses for $Z = 106$ to $Z = 120$. They are due to the Warsaw group of Adam Sobiczewski and his collaborators [2–4]. We are grateful to them for permission to display in this talk those preliminary results, some of which are not published.

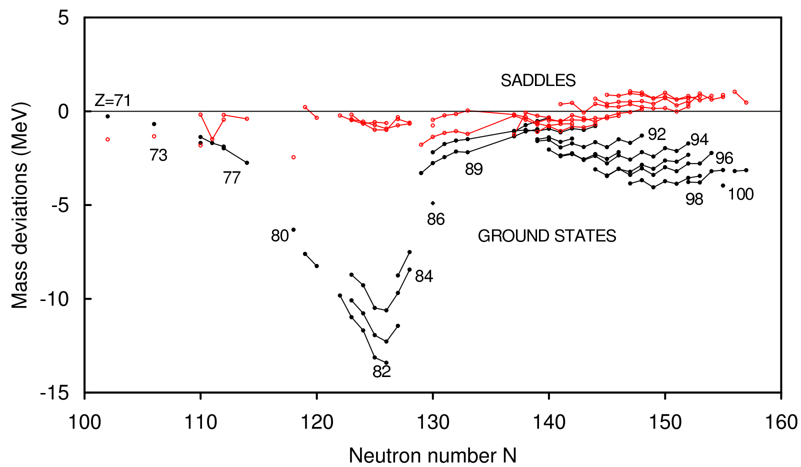

Fig. 1. The black circles represent deviations of measured ground state masses from masses of the spherical configuration, $M_{\mathrm{macro}}(\mathrm{sphere})$, calculated using the Thomas–Fermi theory [6,7]. Isotopes are connected by lines and the labels help to identify the atomic numbers. The red open circles represent deviations of measured saddle masses from calculated saddle masses $M_{\mathrm{macro}}(\mathrm{saddle})$, which were obtained by adding to $M_{\mathrm{macro}}(\mathrm{sphere})$ Thomas–Fermi fission barriers calculated according to [8].

Why am I focusing this talk on nuclear saddle-point masses? These masses control the relative probability for an excited compound nucleus to fission, and a nucleus that fissions gives up any chance of cooling down by neutron and gamma ray emission to form a residual nucleus in its ground state. Avoiding fission in a compound nucleus deexcitation cascade and thus forming new heavy elements and isotopes is an important way of improving our understanding of nuclear structure and nuclear reactions. A difference of 1 MeV in the saddle point mass can make the difference between success and failure in experiments aimed at making new heavy nuclei.

I will remind you presently of the standard way of estimating the relative probability (usually written as the ratio of relative decay widths $\Gamma_n/\Gamma_{\rm f}$) for a nucleus to emit a neutron rather than fission, and of the crucial role of the saddle-point mass in this ratio. But, even without any theory, Fig. 1 teaches us a useful lesson. Thus, to estimate a saddle-point mass to within about 1 or 2 MeV is much easier than to estimate the ground-state mass. You simply use a (good) macroscopic theory and forget about shell effects! (At least that would be the case in the range $Z = 71$ to $Z = 100$.)

If you need an accuracy better than 1 MeV — and, unfortunately, this is often the case — then you have to estimate the relatively small residual shell effects at the saddle point. In this talk I will describe our attempts to make progress with this problem.

2. About $\Gamma_n/\Gamma_{\rm f}$

The canonical "Transition state theory" of chemical reactions was developed in the thirties and adapted by Bohr and Wheeler in 1939 to nuclear fission, in particular to estimating the relative probability of an excited nucleus decaying in two distinct ways, by overcoming two distinct saddle points in deformation space, for example those associated with fission and neutron emission. It gives for the relative probability of emitting a neutron rather than fissioning the elementary relation

$$\frac{\Gamma_n}{\Gamma_{\rm f}} = \frac{N_n}{N_{\rm f}}\,, \tag{1}$$

where N_n and $N_{\rm f}$ are the numbers of levels (decay "channels") available to the neutron and fission saddle point configurations (the "transition states") in the energy (or mass) slots between the total mass of the excited nucleus and the masses of the respective saddles. (The mass of the excited nucleus is equal to the sum of the masses of the reacting partners plus the mass equivalent of the center of mass collision energy in the reaction.) Note that, as discussed with reference to Fig. 9 in [5], the above energy slot in the case of fission does not require a knowledge of the fission barrier height. Only the saddle point mass itself, say $M_{\rm f}$, is needed. This is why in the present talk I am focusing on how to estimate this mass.

3. Nuclear saddle point masses

Coming back to Fig. 1 the solid and open circles are, as I mentioned, the deviations of measured masses from smooth reference mass surfaces $M_{\rm macro}$(sphere) and $M_{\rm macro}$(saddle), respectively. To be precise, $M_{\rm macro}$ (sphere) is the mass of a spherical nucleus calculated using the macroscopic, semi-classical, self-consistent Thomas–Fermi theory (with empirical even–odd corrections included) as described in [6, 7]. It is a mass surface such that, after adding to it shell effect corrections determined (except for very light nuclei) by Möller and Nix using the Strutinsky method, measured ground-state masses for N, $Z \geq 8$ are reproduced to better than 1 MeV on the average. $M_{\rm macro}$(saddle) is the saddle-point mass obtained by adding to $M_{\rm macro}$(sphere) the fission barriers calculated using the above Thomas–Fermi theory [8]. (Thus $M_{\rm macro}$(saddle) has the same even–odd correction in it as $M_{\rm macro}$(sphere).)

It is also instructive to display the measured saddle point masses with reference to the masses $M_{\rm macro}$(sphere) rather than $M_{\rm macro}$(saddle). The upper set of points in Fig. 2 shows the result. These points may now be considered as representing the heights of fission barriers that would have to be added to $M_{\rm macro}$(sphere) in order to reproduce the experimental saddle point masses. They can be compared with the curve in Fig. 2, which is the fission barrier calculated using the Thomas–Fermi theory [8]. The differences between the points and the curve, shown as triangles, are identical with the open circles in Fig. 1, except that they are displayed as functions of the

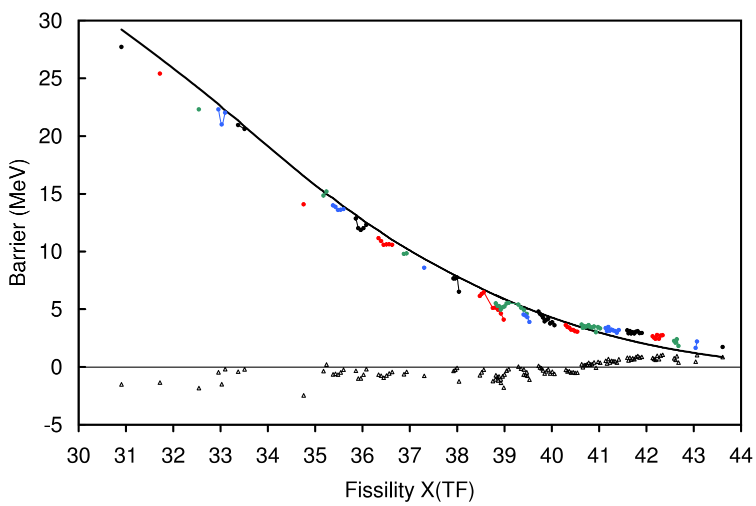

Fig. 2. The upper set of points represents measured saddle masses minus $M_{\rm macro}$(sphere) (see caption to Fig. 1). The curve is the calculated Thomas–Fermi fission barrier, equal to $M_{\rm macro}(\text{saddle}) - \text{M}_{\rm macro}(\text{sphere})$. The triangles display the deviations of the upper points from the curve. They are identical to the red open circles in Fig. 1. The plot is against the Thomas–Fermi fissility X(TF), defined as $Z^2/A(1 - kI^2)$, where $k = 1.9 + (Z - 80)/75$ and $I = (N - Z)/A$.

fissility $X(\mathrm{TF})$ rather than of the neutron number N. [The fissility $X(\mathrm{TF})$ in Fig. 2 is equal to $Z^2/A(1-kI^2)$, where $k = 1.9 + (Z-80)/75$ and $I = (N-Z)/A$ [8]. This $X(\mathrm{TF})$ is a scaling factor (analogous to the scaling factor Z^2/A in the simple Liquid Drop model) which was found to reduce, to a good approximation, the two-variable Thomas–Fermi barriers $B(N,Z)$ to a one-variable function $B(X)$.]

Figs. 1 and 2 show that the Thomas–Fermi theory reproduces the measurements to within about 1 or 2 MeV. The deviations scatter around -1 MeV for $N < 136$ (*i.e.*, $X(\mathrm{TF})$ less than about 40) and then increase systematically to about $+1$ MeV for $N > 136$.

With one reservation, the black circles in Fig. 1 may be regarded as experimentally determined ground state shell effects for the nuclei in question, and the red open circles as the shell effects in the corresponding saddle point configurations, the focus of our attention. The reservation is that, although the points in Figs. 1 and 2 originated in purely experimental ground state and saddle masses, they are displayed as differences between these masses and reference mass surfaces $M_{\mathrm{macro}}(\mathrm{sphere})$ and $M_{\mathrm{macro}}(\mathrm{saddle})$ that do depend on theory. This reservation notwithstanding, the striking feature of Fig. 1 is how much smoother the measured saddle point masses are compared to the ground state masses. We believe this is due, in large measure, to the following "topographic theorem".

4. The topographic theorem

The topographic theorem (see Appendix C in [6]) explains why nuclear saddle point masses are so much smoother than ground state masses. The theorem relies for its validity on the relatively short range of shell effect oscillations that are superposed on the macroscopic deformation energy landscape. On general grounds (see Section 4 in [9] as well as [10]) the range of shell oscillations is of the order of magnitude of the wavelength of the fastest particle in the nucleus, the Fermi wavelength $\lambdabar_{\mathrm{F}}$. This is a constant, and its ratio to the range of characteristic macroscopic deformations is $\lambdabar_{\mathrm{F}}/(\text{nuclear radius})$, *i.e.*, $\sim A^{-1/3}$. This is formally a small quantity.

The physical content of the topographic theorem can be appreciated by imagining a large sheet of egg packaging material, or a foam-rubber sheet consisting of short range bumps and dimples (representing shell effects), deformed into a gently curving overall saddle shape (or ridge). In trying to cross this dimpled saddle from one low region to the other in the most economical manner, it clearly does not pay to go over a bump in the saddle region. But it also does one no good to go into a hollow there, since one then needs to come out of it again. So in the end the optimum path will avoid bumps and will ignore hollows. Hence, the mass of the saddle point will be close to what it would have been in the absence of the shell oscillations, *i.e.*, in the macroscopic approximation. The striking thing about this conclusion is that it is true even though there *are* appreciable shell effects in the immediate neighborhood of the saddle point. This topographical expectation finds experimental confirmation in the saddle masses displayed as barrier heights (the open circles) in Fig. 2 and in the saddle mass deviations (the triangles), which are smoother by an order of magnitude than the ground state deviations (the solid circles in Fig. 1). Note that the remaining deviations from smoothness in the saddle masses are significantly smaller than typical calculated shell effects in the saddle region.

The statement that the topographic theorem predicts saddle masses close to saddle masses calculated macroscopically needs to be qualified for very heavy nuclei, for which the macroscopic fission barrier has vanished and the macroscopic deformation energy is a monotonically decreasing function of the fission degree of freedom. In those cases the formal continuation with increasing fissility of macroscopic saddles actually leads to *oblate* saddles, quite irrelevant to actual saddle points that are due entirely to shell effect dimples in (generally) prolate or spherical configurations. The topographic theorem (based on the avoidance of bumps in the deformation energy landscape) should then be understood to imply that the saddle mass associated with climbing out of the dimple may be estimated as the macroscopic mass a little beyond the location of the dimple, where the dimple would be turning into a bump. For an attempt to implement this idea see Appendix B.2 in [5]. The above extension of the topographic theorem becomes relevant in the case of the theoretical saddle masses for $Z \geq 106$, to be considered next.

5. Theoretical saddle masses of nuclei with $Z \geq 106$

Fig. 3 shows the deviations of calculated ground state and saddle masses, deduced from [2–4] (and adjusted by us to remove even–odd staggering) from a smooth mass surface $M_{\rm macro}$(sphere), analogous to (but, of course, not identical with) the $M_{\rm macro}$(sphere) in Section 3. The plot is similar to Fig. 1, but the decomposition of the calculated masses into a macroscopic part and a "shell correction" is not quite unambiguous. This is because the calculated mass $M_{\rm calc}$ is given as the sum of the above $M_{\rm macro}$(sphere) and a microscopic part $M_{\rm micro}$, which latter incorporates both the shell correction and the pairing energy (the even–odd staggering) – these are not listed separately.

The empirical adjustment for the even–odd staggering that we applied to the calculated masses may be illustrated with reference to Fig. 4. The full diamonds show, for $Z = 110$, the values of $M_{\rm micro}$. By subtracting $M_{\rm micro}$ from $M_{\rm calc}$ one obtains an essentially smooth mass surface $M_{\rm macro}$(sphere),

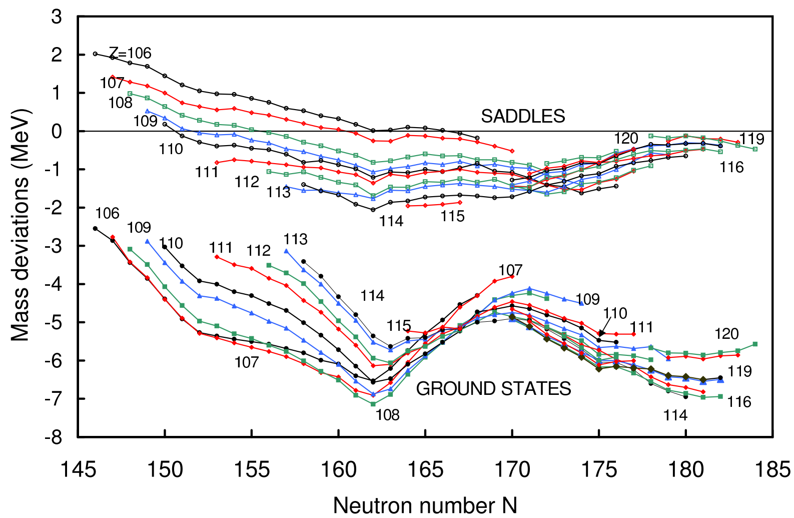

Fig. 3. The lower set of points represents the difference between calculated ground state masses $M_{\rm calc}$ and a smooth macroscopic mass surface $M_{\rm macro}$(sphere). (See text for details.) The upper set of points represents calculated saddle masses minus $M_{\rm macro}$(sphere). The saddle masses are preliminary, since they were calculated under the assumption of axial and reflection symmetry. For both the upper and lower points even–odd staggering was removed, as described in the text. The calculations are those of the Warsaw group [2–4]. Labels refer to atomic numbers and isotopes of an element are connected by lines.

which has neither shell nor even–odd irregularities in it. The open squares in Fig. 4 show the calculated saddle masses minus the above $M_{\rm macro}$(sphere). If such plots of ground state and saddle mass deviations were presented for all Z values in a single figure like Fig. 3, the result would be essentially indecipherable because of the even–odd stagger. We found that one way out was to shift down the ground state odd-A points in Fig. 4 by 9 MeV/$\sqrt{A}$ and the saddle odd-A points by 12 MeV/$\sqrt{A}$ before entering those values in Fig. 3. This made the odd-A and even–even points follow a single trend, which made it possible to construct an intelligible Fig. 3. Note, however, that the absolute values of the resulting mass deviations in Fig. 3 would have been different if the even–even points had been *raised* to match the odd-A points. A third way of removing the stagger would be to raise the even–even and odd-A points to match the trend of presumed odd–odd points, expected to be higher than the odd-A points by another 9 MeV/$\sqrt{A}$ for ground states and by 12 MeV/$\sqrt{A}$ for saddles. This ambiguity in producing a plot like Fig. 3, which was supposed to display shell corrections, is the result of the calculations in question providing only the *sum* of shell and pairing effects.

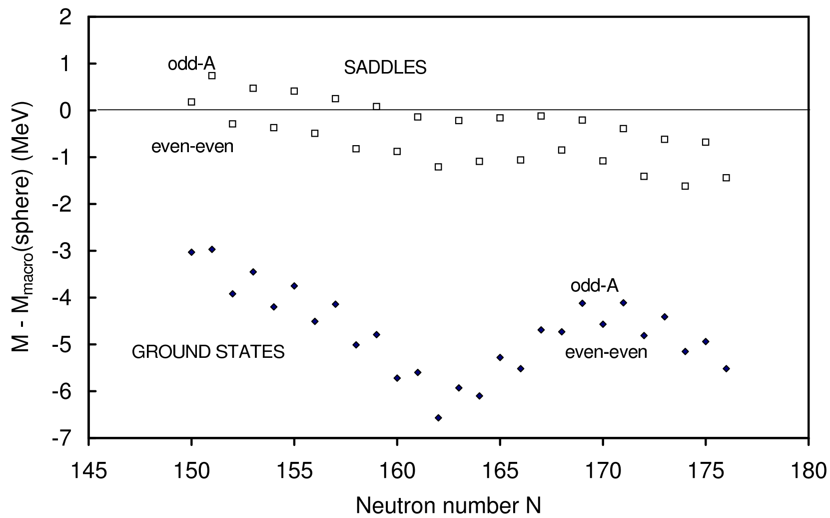

Fig. 4. The solid diamonds represent, for $Z = 110$, the difference between calculated ground state masses and calculated macroscopic masses $M_{\rm macro}$(sphere). The open squares represent the difference between the calculated saddle masses and $M_{\rm macro}$(sphere). An even–odd staggering is visible. In constructing Fig. 3 this staggering was removed by lowering the odd-A ground state masses by 9 MeV/$\sqrt{A}$ and the odd-A saddle masses by 12 MeV/$\sqrt{A}$.

Comparing the upper and lower parts of Fig. 3 one sees again the relative smoothness of the saddle masses compared to the ground state masses. Several words of caution are, however necessary. First, as stressed in [3], the theoretical saddle masses represent preliminary values, obtained with saddle shapes restricted to axial and reflection symmetry. In the example of the nucleus with $Z = 116$, $N = 178$, inclusion of these extra degrees of freedom decreased the saddle mass by 1 MeV [3]. Similar decreases may be expected in other cases.

Second, unlike in Fig. 1, the saddle masses in Fig. 3 are displayed with reference to $M_{\rm macro}$(sphere) rather than $M_{\rm macro}$(saddle), which was not available. For very heavy nuclei the difference between these quantities (the macroscopic fission barrier) tends to zero and may be disregarded. But for progressively lighter nuclei, where the macroscopic fission barriers become appreciable, the above deviations would begin to display mostly the expected increasing macroscopic fission barriers, rather than saddle point shell effects. (Compare Fig. 2.) Unfortunately, we are not in a position to allow for this effect in our plots because the relevant macroscopic fission barriers have not been calculated.

Related to this point is the feature discussed at the end of Section 4. For the very heavy nuclei in Fig. 3 the macroscopic barriers have vanished and the relevant saddle masses are the masses associated with climbing out of a shell effect dimple along a prolate fission path. When the nucleus in question is shell-stabilized in a *deformed* ground state, the saddle will, in general, be located at a sizeable deformation, at which the macroscopic energy can be appreciably below the macroscopic energy of the sphere. The extended macroscopic theorem would then lead one to expect the saddle mass deviations to become increasingly negative with increasing nuclear fissility, as is indeed observed in Fig. 3. On the other hand, for the heaviest nuclei, beyond about $Z = 114$, the ground states become eventually stabilized at the *spherical* shape. The saddle configuration will now be much less deformed, and the macroscopic energy at that deformation will be less negative with respect to the macroscopic energy of the sphere. This would lead one to expect an actual reversal in the trend of the saddle mass deviations with Z increasing beyond about 114, again in agreement with what is observed in Fig. 3. It remains to be seen whether these qualitative expectations are borne out by a quantitative analysis.

6. Summary

It is instructive to combine Figs. 1 and 3 in a single plot, Fig. 5. This plot summarizes information, both experimental and theoretical, concerning the trends in ground state and saddle masses in the range of atomic numbers Z = 71–120 and neutron numbers N = 102–184. As mentioned in Section 5, the theoretical mass deviations should not be taken at face value as representations of shell effects, since some modifications are expected and, in addition, there is present an ambiguity concerning the separation of shell and pairing corrections. The overall message of this compilation is, nevertheless, the relative smoothness of saddle point masses compared to ground state masses. The challenge is to make less ambiguous the remaining irregularities and to provide, if possible, an understanding of their overall features.

There is one practical lesson that we would like to stress. The large number of current numerical studies of masses of heavy and superheavy nuclei, usually list calculated ground state masses and fission barriers (sometimes only one or the other), but do not list or display the saddle point masses themselves. Now ground state masses and fission barriers, taken separately, are "jagged" functions of N and Z, subject to large shell effect irregularities. But their sums, the saddle masses, are much smoother objects, which are easier to parameterize and extrapolate. Bearing in mind that it is the saddle mass for fission, M_{f} , and *not* the fission barrier that is needed in estimating

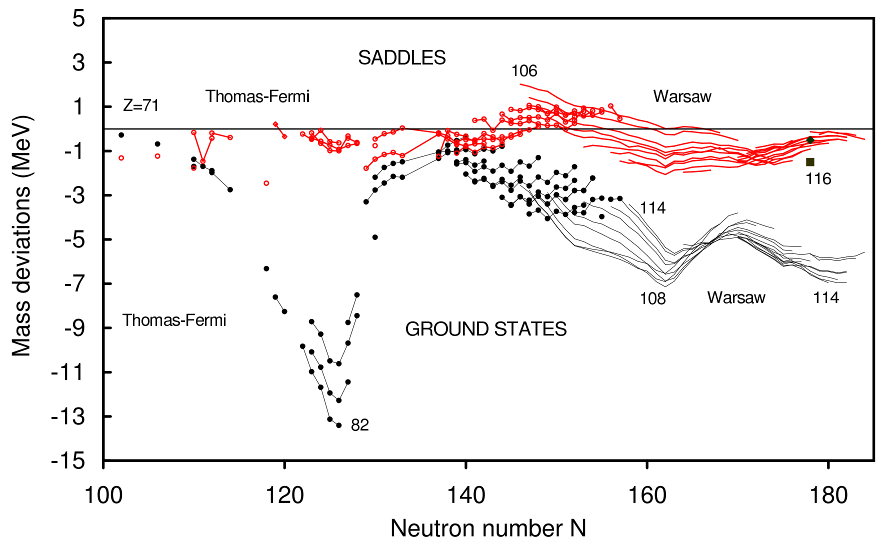

Fig. 5. This figure combines in one plot Figs. 1 and 3. The circle and square labeled 116 illustrate the lowering by 1 MeV of the saddle mass of the nucleus $Z = 116$, $N = 178$, resulting from including in the calculations deviations from axial and reflection symmetry. Note that, as explained in the text, there is some ambiguity in interpreting the calculated mass deviations as due to shell effects.

the relative probability for a nucleus to survive fission, it would be well if M_{f}, a basic datum of fission physics, were accorded the same prominence in the presentation of calculations as the nuclear ground state mass.

An additional plea to those who study nuclear masses using the macroscopic–microscopic approach: please provide the *macroscopic* saddle point masses as well as the saddle masses with shell effects included. Compared to the latter, macroscopic saddle masses are almost trivial to determine, but they are essential for isolating and understanding the nature of the residual shell effects on saddle masses.

We would like to thank I. Muntian, Z. Patyk and A. Sobiczewski for permission to use a number of their unpublished results. We also thank Z. Patyk and A. Sobiczewski for discussions and for performing for us some additional calculations. This work was supported by the U.S. Department of Energy under Contract No. DE-AC0376SF00098 (LBNL) and by the Polish Ministry of Science and Higher Education under Grant MNiSW No. 1 P03B 090 29.

REFERENCES

[1] A. Mamdouh, J.M. Pearson, M. Rayet, F. Tondeur, *Nucl. Phys.* **A644**, 389 (1998).

[2] I. Muntian, Z. Patyk, A. Sobiczewski, *Acta Phys. Pol. B* **32**, 691 (2001); *Acta Phys. Pol. B* **34**, 1359 (2003).

[3] I. Muntian, A. Sobiczewski, *Int. J. Mod. Phys.* **E14**, 417 (2005); *Acta Phys. Pol. B* **36**, 1359 (2005).

[4] Z. Patyk, A. Sobiczewski, private communication.

[5] W.J. Świątecki, K. Siwek-Wilczyńska, J. Wilczyński, *Phys. Rev.* **C71**, 014602 (2005).

[6] W.D. Myers, W.J. Swiatecki, *Nucl. Phys.* **A601**, 141 (1996).

[7] W.D. Myers, W.J. Swiatecki, *Table of Nuclear Masses according to the 1994 Thomas–Fermi Model*, Lawrence Berkeley Laboratory report LBL-36803, December 1994. Accessible on `http://ie.lbl.gov/txt/ms.txt`.

[8] W.D. Myers, W.J. Swiatecki, *Phys. Rev.* **C60**, 014606 (1999).

[9] W.D. Myers, W.J. Swiatecki, *Nucl. Phys.* **81**, 1 (1966).

[10] A. Bohr, B.R. Mottelson, *Nuclear Structure*, Vol. II, Benjamin, New York 1975, pp. 136, 605.